

COMPUTING SIMILARITY FROM MULTIPLE INPUT VOLUMES – PROGRAM similarity_multiple_input

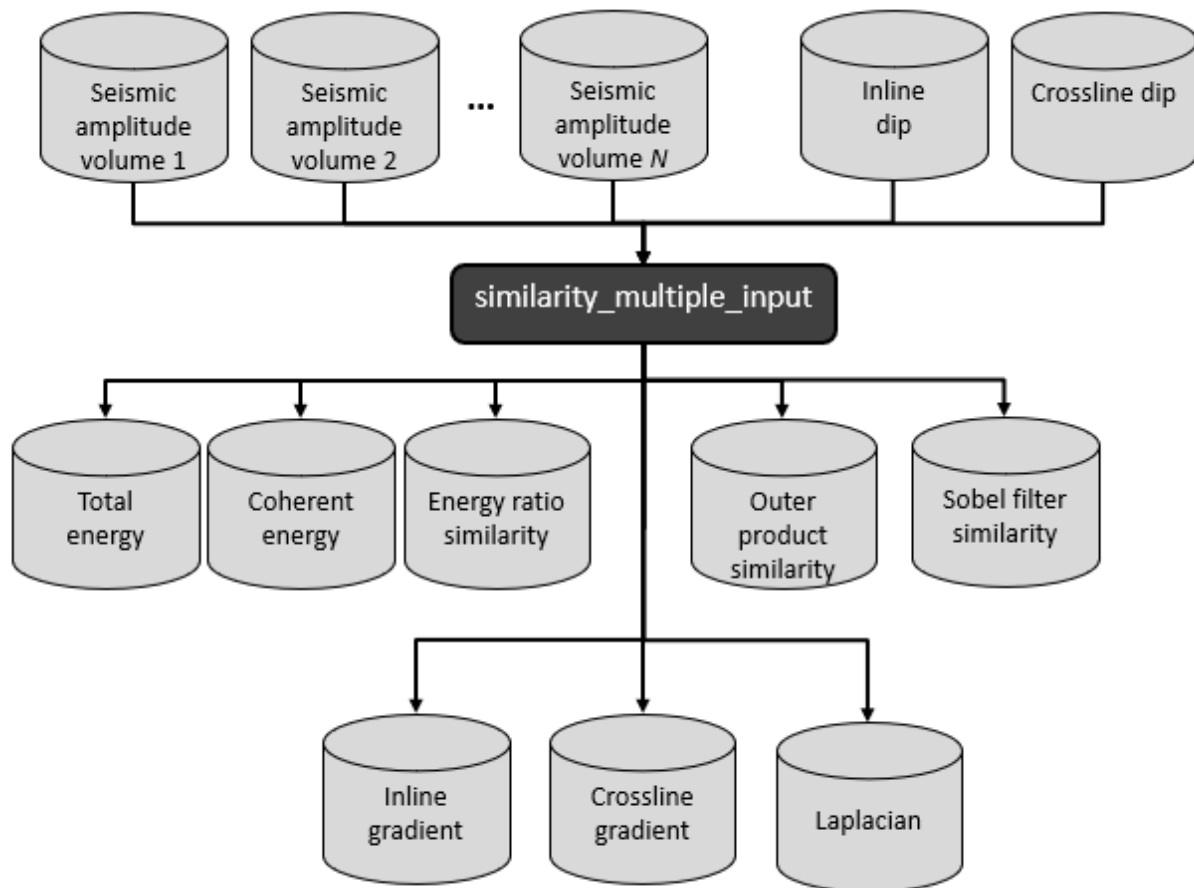
Contents

Computation flow chart.....	1
Computing similarity attributes from multiple input volumes.....	2
The primary Parameters Tab	5
The Analysis window parameter Tab.....	5
The Parallelization Parameters Tab	5
Execution.....	6
Theory: Computing the covariance matrix for multiple input volumes	6
Example:.....	7
References	9

Computation flow chart

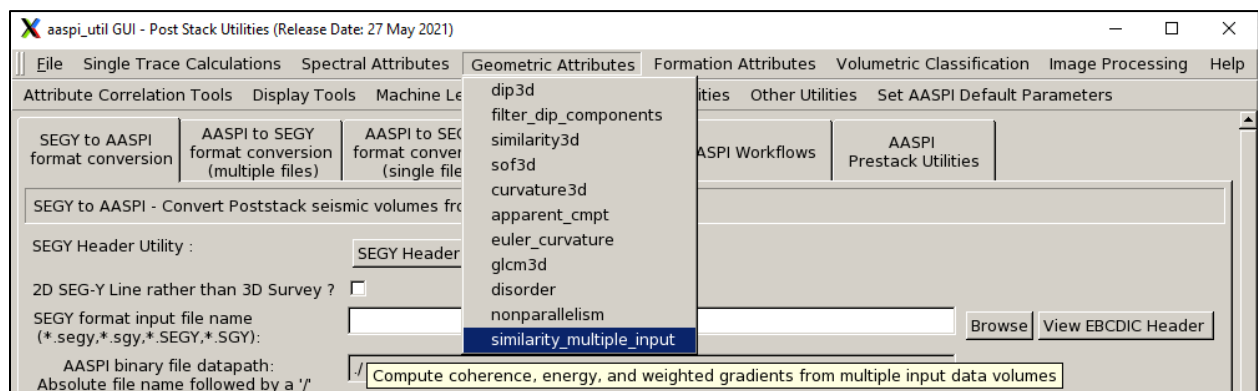
Program **similarity_multiple_input** provides superior results when applied to multiple 3D data volumes that may be azimuthally-, offset-, frequency-limited, or different combinations of azimuthally-, offset- and frequency-limited. The **Similarity_multiple_input** coherence algorithm is based on the **prestack_similarity** program and the **similarity3D** algorithm, which computes the ratio of coherent energy of seismic trace and total energy of seismic trace. The difference compared with other two programs is that in the **similarity_multiple_input** program, the inputs are multiple 3D seismic volumes.

Geometric_Attributes: Program **similarity_multiple_input**

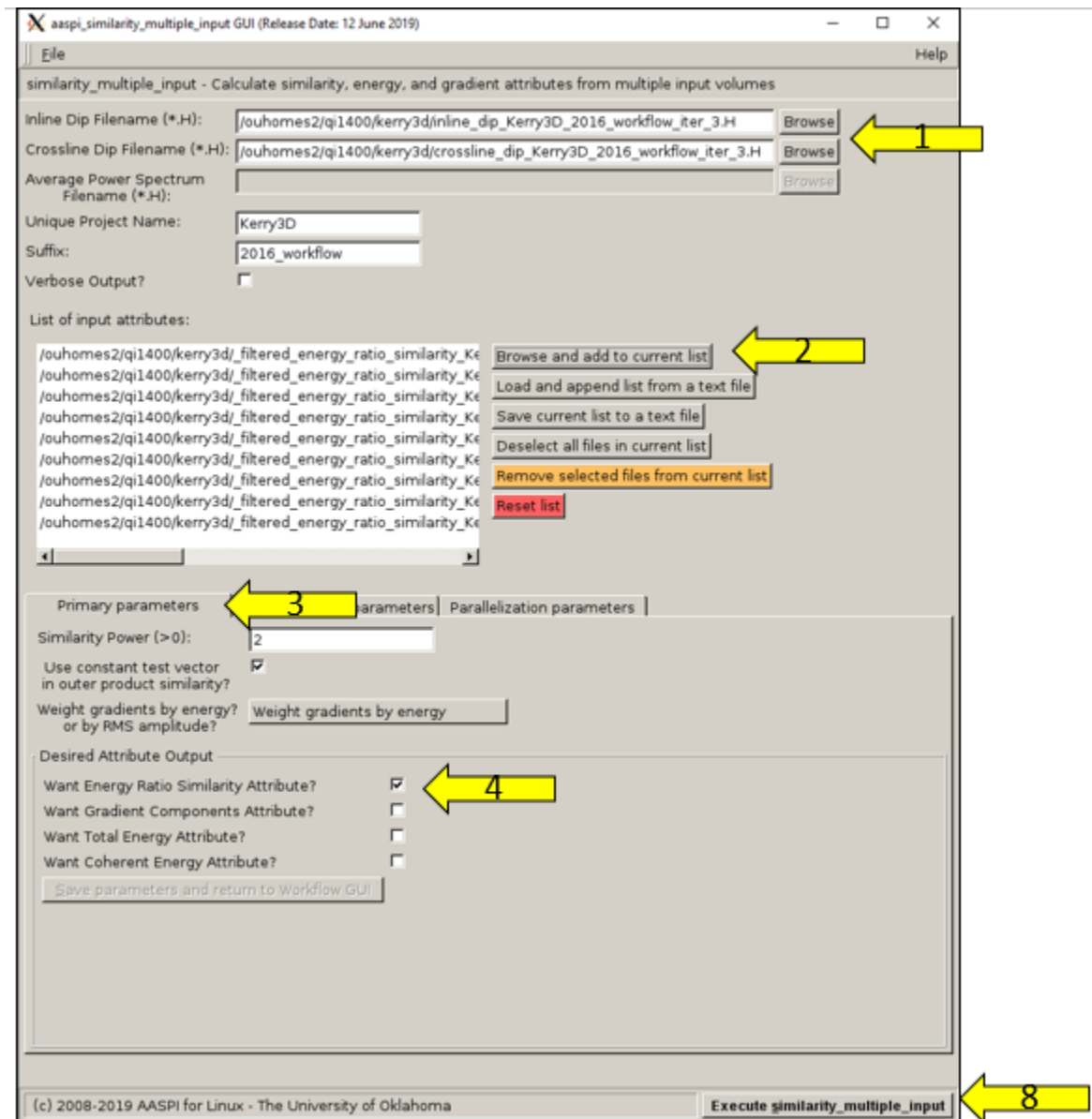


Computing similarity attributes from multiple input volumes

Program **similarity_multiple_input** is found under the *Geometric_Attributes* tab.



Geometric_Attributes: Program **similarity_multiple_input**



Geometric_Attributes: Program **similarity_multiple_input**

Primary parameters | Analysis window parameters | Parallelization parameters

Analysis Window Definition Parameters

Use data-adaptive analysis windows? Use a fixed-size window

Covariance Window Half Height (s): 0.02

Taper applied to vertical analysis window (Percent): 20

Balance data vectors before computing covariance matrix? ☐

Percentile of average magnitude spectrum to define data-adaptive windows: 80

Inline Window Radius (m): 49.9607

Crossline Window Radius (m): 49.993

Use rectangular analysis window? ☒

Primary parameters | Analysis window parameters | Parallelization parameters

Help - Parallelization

Use MPI: ☒

Processors per node: 2 Determine Maximum Processors on localhost

Node list (separated by blanks): localhost

Build an LSF Script? Do Not Run Under LSF

Build a PBS Script? Do Not Run Under PBS

Build a SLURM Script? Do Not Run Under SLURM

Maximum LSF run time (hrs): 10

Maximum number of processors per node: 40

Available batch processors: 2

Determine Optimum Number of Batch Processors

Batch Queue:

(c) 2008-2019 AASPI for Linux - The University of Oklahoma Execute similarity_multiple_input

Click (1) *Browse*, and select *inline and crossline dip components* computed from the poststack seismic amplitude volume by Program **dip3d**. (2) Select multiple 3D seismic data with limited offset, azimuth, or frequency bands. Inputting azimuthally limited 3D seismic volumes results in multi-azimuth coherence. Inputting offset-limited 3D seismic volumes results in multi-offset coherence – and inputting different frequency band spectral voices results in multispectral coherence. If you have a few azimuthally limited seismic volumes, you need to combine these to be one 4D volume. Then you can select if using the average power spectrum, which is an advanced option that allows the definition of a data adaptive analysis window, may be useful for

Geometric_Attributes: Program **similarity_multiple_input**

depth-migrated data where the dominant wavelength changes significantly from shallow to deeper depths. For now, use a fixed window. Don't forget to select unique project name and suffix.

The primary Parameters Tab

(3) Similarity values will range between 0 and 1, with most of the values biased towards 1. If one takes the power of the similarity, the distribution moves towards zero, providing improved contrast in the resulting image. This option remains from a time when many workstation software programs had only limited color bar manipulation capabilities. In a modern system it makes no difference whether one maps nonlinearly (powers), the similarity and plots it against a linear gray scale color bar, or if one plots the unscaled similarity against a nonlinear gray scale color bar. Whether or not you wish to balance the covariance matrix sample vectors prior to constructing it (see the appropriate Theory box below).

The Analysis window parameter Tab

The image below shows the GUI when the Analysis window parameters tab has been selected. By default, **similarity3d** will use (5) a fixed-size analysis window. We will investigate what happens if we toggle this button shortly. For now, define the covariance window half height, percent tapers applied to the samples vertically. Drop down to (6) the inline and crossline window radii. The default will be ± 1 trace in each direction, which for the justin survey are 110 ft and 110 ft. The default is also to use a rectangular vs. an elliptical analysis window. For small windows like this, the rectangular window provides more robust estimates of inline and crossline coherent energy gradient components. For larger elliptical or circular windows, this is less important.

The Parallelization Parameters Tab

The parallelization parameters tab for **similarity_multiple_input** is the same for all AASPI applications. One can run across multiple processors and cores on a single node, across nodes if that is allowed by your IT department, or on large batch supercomputers using LSF, PBS, or SLURM scripts. Details on parallelization can be found in the parallelization section of the documentation *Overview: AASPI Software Parallelization*. **similarity_multiple_input** uses a stencil-based parallelization scheme; this results in suboptimal performance for surveys that do not approximate a rectangular shape, where cores assigned to dead or padded traces lie idle.

Execution

After selecting all the parameters you wish to change, click (8) Execute **similarity_multiple_input** and generate several output files:

```
energy_ratio_similarity_Kerry3D_2016_workflow_multiple_input.H  
energy_ratio_similarity_Kerry3D_2016_workflow_multiple_input.H@@
```

We only compute **energy_ratio_similarity**, and the program generates 1 output volume. The volume is multiazimuth coherence volume (because we input 8 azimuthally-limited seismic amplitude volumes) that has a suffix *m* at the middle of output name. The below box indicates algorithm part of this multiazimuth coherence. The details of multiazimuth coherence algorithm can be found in publication *Qi et al. (2017)*.

Theory: Computing the covariance matrix for multiple input volumes

The covariance matrix is constructed from a suite of sample vectors that are parallel to structural dip. The covariance matrix for this analysis window is

$$C_{mn} = \sum_{k=-K}^{+K} (d_{km}d_{kn} + d_{km}^H d_{kn}^H),$$

where the superscript H denotes the Hilbert transform along traces, and the subscripts m and n are indices of input traces (1, 2, ..., M). For example, the element C_{23} in the covariance matrix C_{mn} is $\sum_{k=-K}^{+K} (d_{k2}d_{k3} + d_{k2}^H d_{k3}^H)$. The Hilbert transform (90° phase rotated) version of the data does not modify the vertical resolution, but improves areas of low SNR about zero crossing (Marfurt, 2006). The first eigenvector $v(1)$ of the covariance matrix C best represents the lateral variation of each sample vector of the constituent.

We generalize the concept of energy-ratio coherence by summing J covariance matrices $C(\phi_j)$ computed from each of the J azimuthally-, offset-, frequency-sectored data volumes:

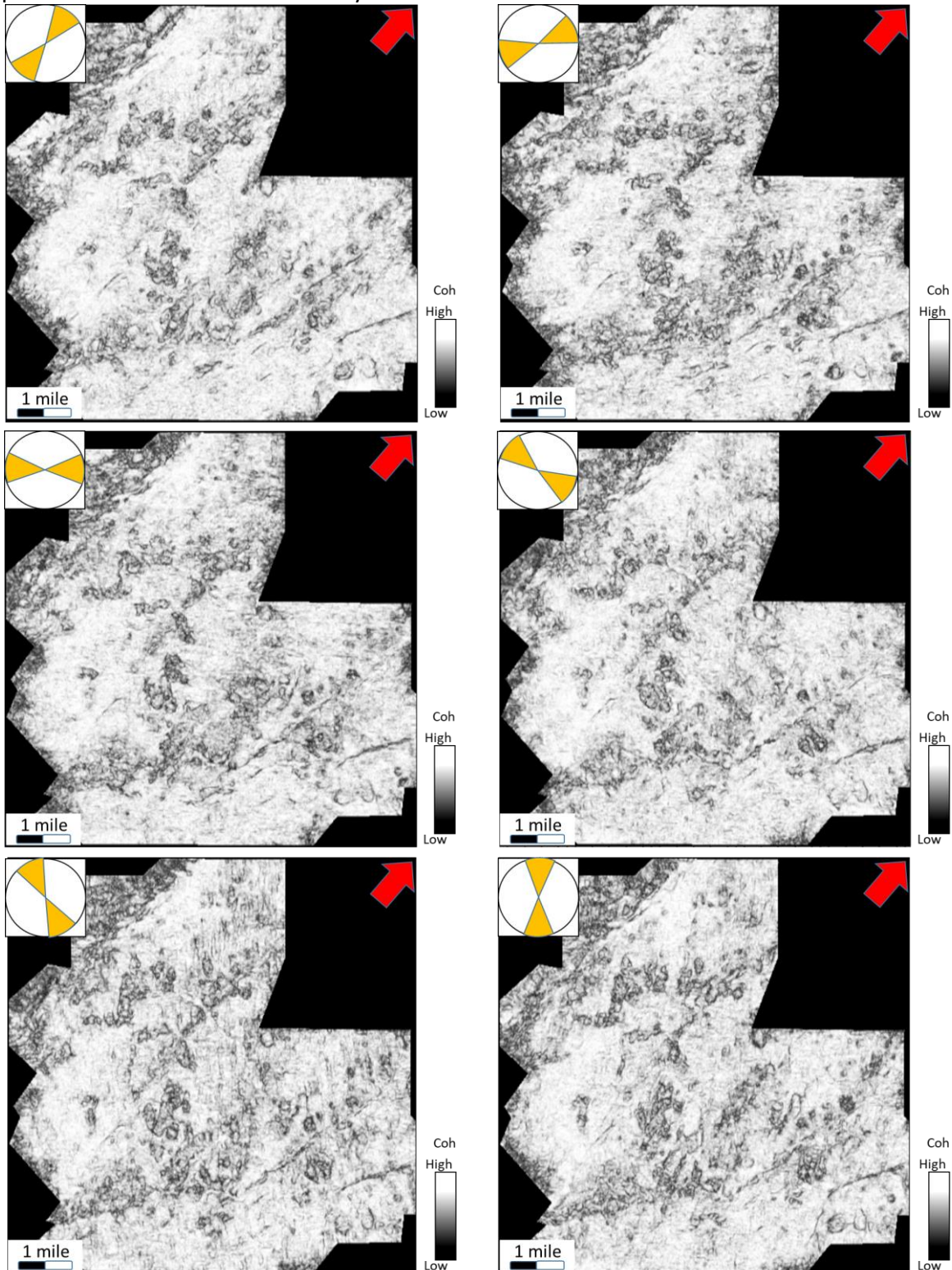
$$C_{multi-\phi} = \sum_{j=1}^J C(\phi_j).$$

The summed covariance matrix is of the same M by M size as the original single-component covariance matrix but is now composed of J times as many sample vectors. As the conventional covariance matrix, the multi-component covariance matrix is a symmetric positive definite matrix. Eigen-decomposition of the multi-component covariance matrix is a nonlinear process, such that the first eigenvector of the summed covariance matrix is not a linear combination of the first eigenvectors computed for the azimuthally limited covariance matrices, in which case the resulting coherence would be the average of the azimuthally limited coherence computations.

Geologic details in each azimuthally seismic image are transferred into sample vectors. Summing sample vectors provides a means of summing geologic anomalies into the multi-azimuth covariance matrix, such as stacking up azimuthally limited coherence. This nonlinear Eigen-decomposition of the multi-azimuth covariance matrix has advantages in suppressing random noise that would help deal with random noise in azimuthally limited seismic volumes. To lessen computation cost, azimuths are commonly binned into six 30° or eight 22.5° sectors, although finer binning is common in large processing shops.

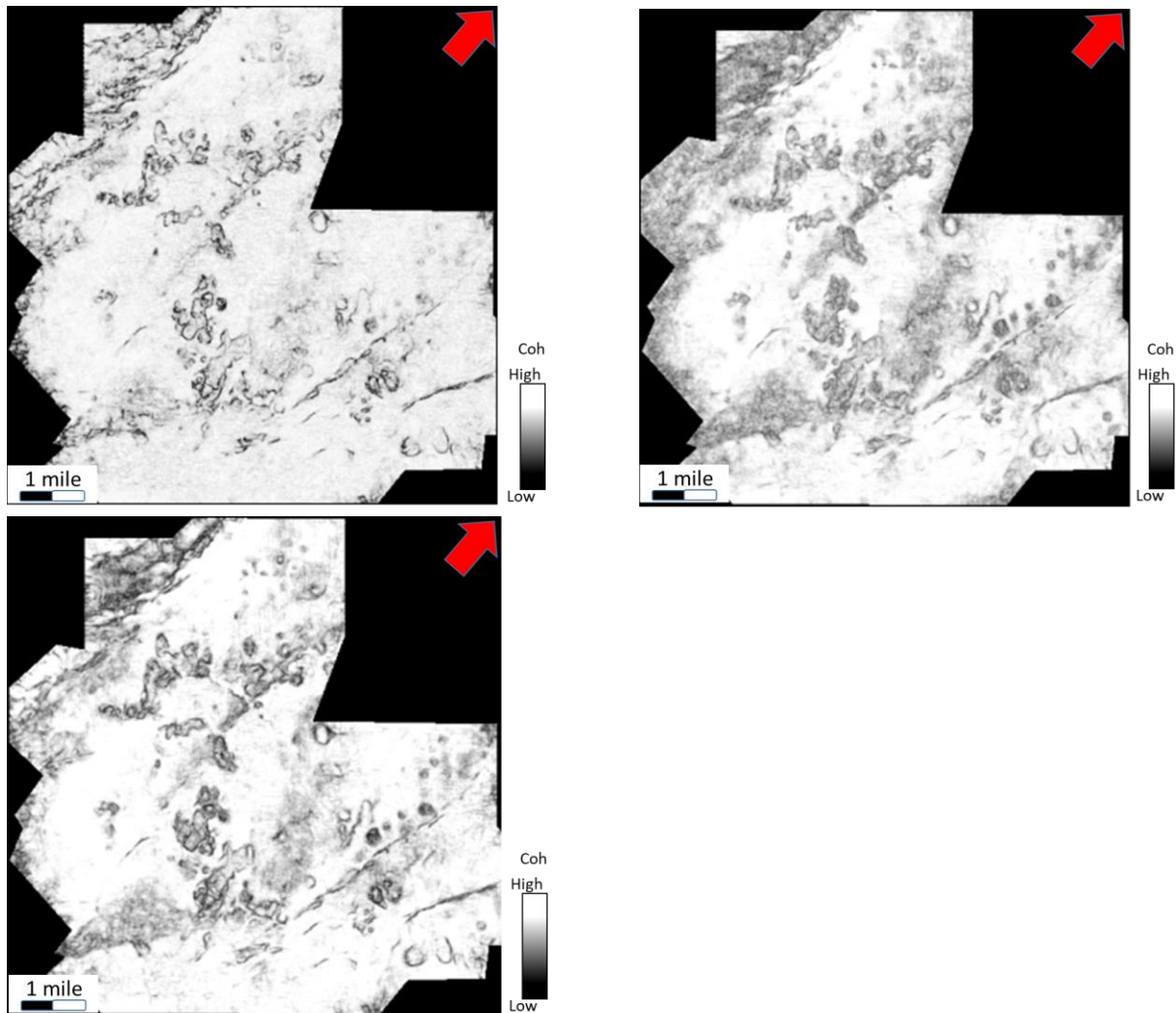
Example:

We can plot our outputs to QC the results by clicking (1) the AASPI QC Plotting tab in the **aaspi_util** GUI. Time slices at $t=0.74$ s through the six different azimuthally limited seismic amplitude volumes of the test survey looks like:



Geometric_Attributes: Program **similarity_multiple_input**

Stacking the six seismic amplitude volumes and then computing coherence (the conventional analysis workflow) gives the result shown in the bottom left figure. This image shows increased SNR but slightly lower lateral resolution than the azimuthally limited coherence time slices shown in azimuthally limited coherence images. The right figure shows the result of stacking the six images shown in azimuthally limited coherence images. The resolution on stacked coherence is lower than that of post-stack coherence; however, edges of the karst features appear more pronounced than on the traditional coherence computation. The third figure shows the multi-azimuth coherence result computed using the covariance matrix. Note that the multi-azimuth coherence displays the higher spatial resolution than either traditional coherence or the stacked azimuthal coherence.



References

Chopra, S., and K. J. Marfurt, 2019, Multispectral, multiazimuth, and multioffset coherence attribute applications: Interpretation, 7, SC21-SC32. DOI 10.1190/INT-2018-0090.

Qi, J., F. Li, and K. J. Marfurt. 2017, Multiazimuth coherence: Geophysics, **82**, o83-o89.

Lyu, B., J. Qi, F. Li, Y. Hu, T. Zhao, S. Verma, and K. J. Marfurt, 2020, Multispectral coherence – Which decomposition should we use?: Interpretation, **8**, T115-T129.